

**N79-19040**

Paper No. 32

**ABLATIVE PERFORMANCE OF CARBON-CARBON NOSETIPS  
IN SIMULATED RE-ENTRY ENVIRONMENTS**

*D. E. Nestler, General Electric Company, Re-Entry and Environmental  
Systems Division, Philadelphia, Pennsylvania*

**ABSTRACT**

A summary is presented of ablation performance data for carbon-carbon nosetip models obtained over a range of pressures from 10 to 168 atm. Two classes of tests are reviewed: (1) steady state, in which a constant environment is imposed on the model, and (2) ramp, in which the pressure is increased from 10 to 80 atmospheres to simulate re-entry pressure history.

Steady state recession rates which differ by a factor of two for a given material over the pressure range tested are shown to be compatible with the JANAF thermochemical theory for graphite, provided that an augmentation of turbulent heating due to surface roughness is introduced.

Ramp tests are used to deduce the pressure at which boundary layer transition occurs, from photographic observation of gouging due to turbulent heating. Different camera views, as well as post-test evaluation, show that boundary layer transition on 3-D carbon-carbon is not uniform; transition occurs earlier at 45 degrees between the orthogonal weave axes.

Comparison of arc test parameters with typical re-entry vehicle parameters is included, to assess the adequacy of the test simulation. Based on this comparison, recommendations are made for facility developments which would yield improved simulation capability for re-entry vehicle nosetip ablative performance.

**INTRODUCTION**

Three-dimensional weaves of carbon-carbon are prime contenders for nosetips of future re-entry vehicles. The 3-D carbon-carbon material can provide ablative performance comparable to that of graphite, but with superior mechanical properties.

It has become current practice to test advanced carbon-carbon nosetip materials in high pressure arcs to determine their relative ablative performance prior to flight-testing selected candidate materials. Two types of tests are commonly conducted: (1) steady state, in which a constant environment is imposed on the model, and (2) ramp, in which the pressure is steadily increased by advancing the model towards the nozzle exit.

The objective of this paper is to present the results of evaluations of selected arc test data of carbon-carbon nosetip models, including an assessment of the adequacy of the test simulation.

#### NOMENCLATURE

B	dimensionless blowing parameter; $B' = \frac{\dot{m}}{C_h}$
$C_h$	heat transfer coefficient for actual surface
$C_{h0}$	heat transfer coefficient for smooth surface
E	Euler number; $E = \frac{S dU_e}{U_e dS}$
$H_{CL}$	centerline enthalpy of arc flow
$H_s$	enthalpy of solid particles being mechanically removed from ablating surface.
$H_w$	wall enthalpy
K	surface roughness
$\dot{m}_m$	thermomechanical mass loss rate
$\dot{m}_{TC}$	thermochemical mass loss rate
Pr	Prandtl number
p	local static pressure
$P_s$	stagnation pressure
$q_c$	convective heat flux
$q_{RR}$	reradiative heat flux
$q_T$	turbulent convective heat flux
$Re^*$	local sonic point unit length Reynolds number; $Re^* = \rho_e U_e / \mu_e$
S	wetted surface length measured from stagnation point
$\dot{s}$	steady state recession rate
$T_e$	static temperature at edge of boundary layer
$T_w$	wall temperature
Tu	turbulence level
$U_e$	velocity at edge of boundary layer
$\beta$	cone half angle
$\epsilon T$	compressibility correction in turbulent heat flux relation
$\mu_e$	absolute viscosity at edge of boundary layer
$\rho_e$	density at edge of boundary layer
$\theta$	momentum thickness of boundary layer

## STEADY STATE TESTS

The two facilities most frequently used for steady state tests are the 50-megawatt arc of the Air Force Flight Dynamics Laboratory and the HIP facility of the MacDonnell-Douglas Research Laboratory. In the 50-megawatt arc, initially spherical-nose models sharpen to a biconic shape (Figure 1A) with a quasi-steady state turbulent recession rate. In the HIP facility, the models are initially biconic, and retain their turbulent shape during exposure (Figure 1B). Nominal test conditions for steady state tests in these facilities are given below:

FACILITY	PRESSURE (ATM)	ENTHALPY		MODEL DIAM.	
		(kj/kg)	(btu/lb)	(cm)	(in.)
50 MW Arc	80	11600	5000	1.27	0.50
HIP	124	6914	3000	0.762	0.30
HIP	168	8027	3800	0.762	0.30

The enthalpy values quoted are flow centerline values which are inferred from calorimeter heat flux measurements as required to match theory, and tacitly assume no heat transfer augmentation due to free stream turbulence in the arc flow.

Centerline recession history corresponding to Figure 1A is shown in Figure 2. Average recession rates are determined from such plots for the quasi-steady or equilibrium ablated shape.

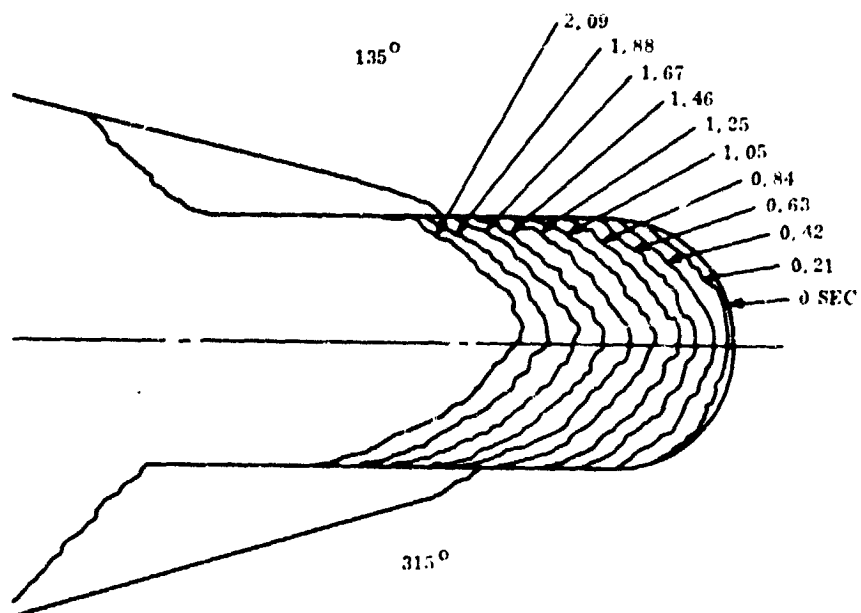
Recession rates for identical carbon-carbon models were correlated empirically with test conditions for a range of pressure from 80 to 168 atmospheres (Figure 3). The correlating parameter employs exponents of 0.8 and 0.2 on stagnation pressure and model diameter, respectively, since these exponents appear in simple turbulent boundary layer heat flux theory.

It is relatively straightforward to show qualitatively by means of the graphite thermochemical response models that an increase in the value of  $H_{CL}$  or  $p_s$  from one steady state run to another will cause an increase in steady state recession rate  $\dot{S}$ . The derivation of an explicit proportionality expression relating  $\dot{S}$  to  $H_{CL}$  and  $p_s$  is not straightforward, however, due to the complex variation of the mass loss rate parameter  $\beta$  with pressure and wall temperature (Figure 4).

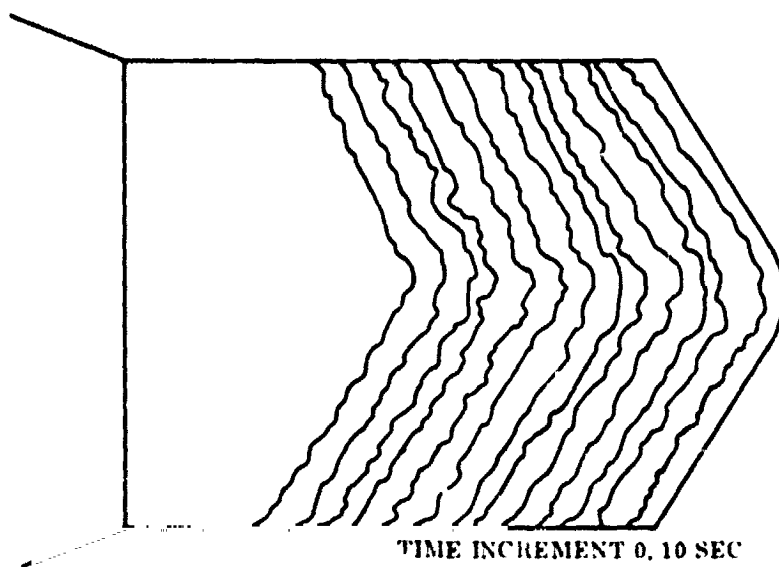
In the 50 MW or HIP high pressure arc environments, the heat flux is so high that the surface temperature is driven to the sublimation regime. In a steady state test,  $T_w$  is determined by the steady state energy balance:

$$0 = \dot{q}_c - \dot{q}_{RR} - \dot{m}_T H_w - \dot{m}_s H_s \quad (1)$$

FIGURE 1. TYPICAL SHAPE CHANGE HISTORIES



A. 50 MW Arc - 80 Atm.



B. HIP - 124 Atm.

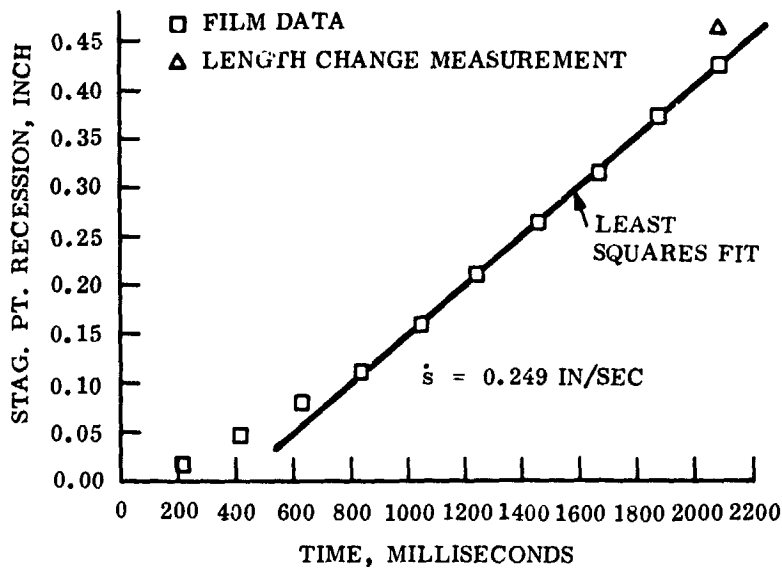


FIGURE 2. Typical Recession Rate Determination (50 MW Test)

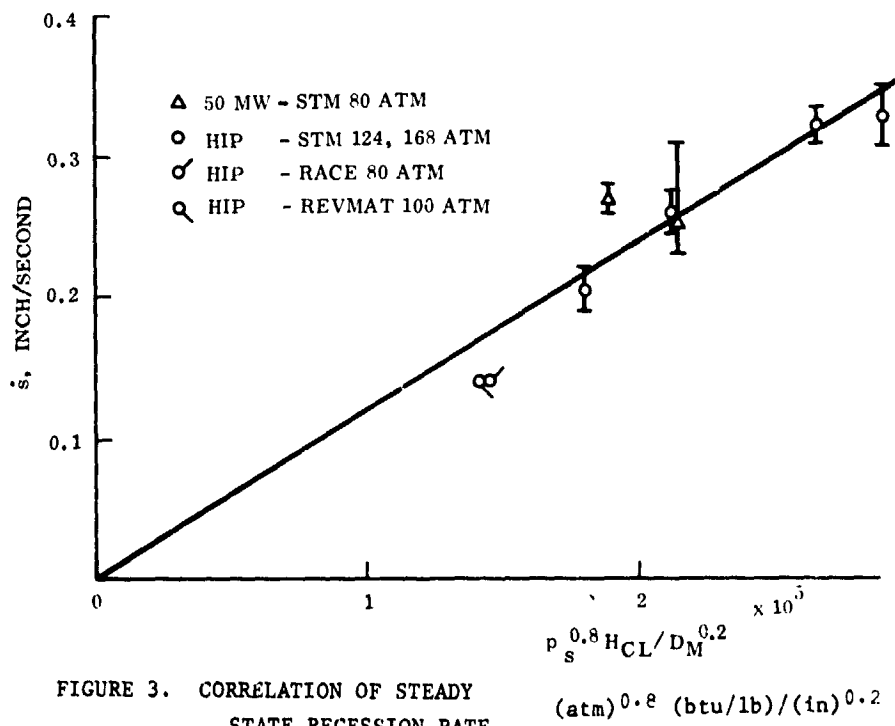


FIGURE 3. CORRELATION OF STEADY STATE RECESSION RATE

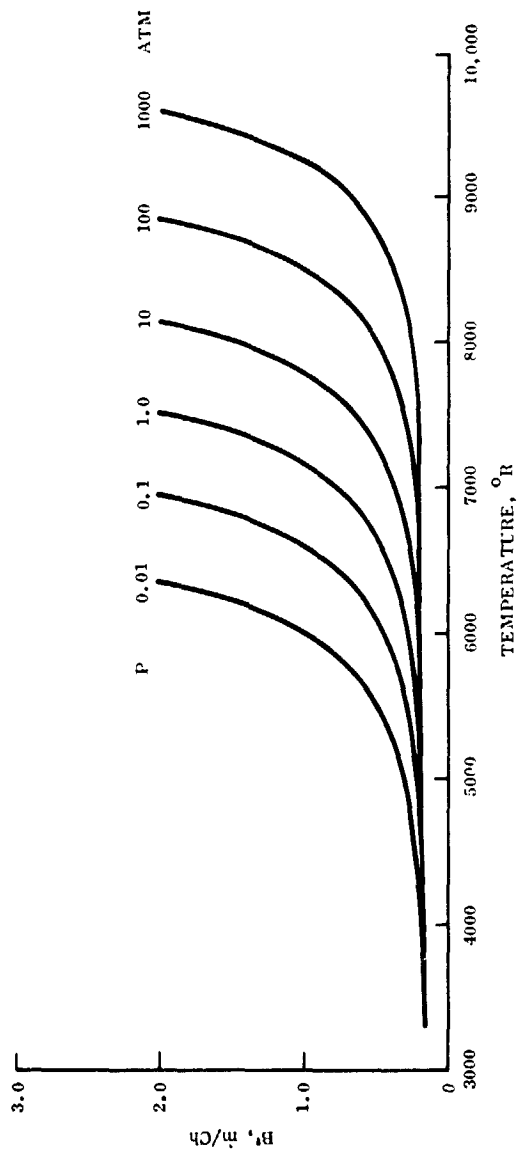


FIGURE 4. Graphite Mass Loss Rate for JANAF (Aerotherm) Thermochemistry

Neglecting thermomechanical mass loss rate  $\dot{m}_M$ , Eq. (1) may be written as:

$$\dot{q}_c = \dot{q}_{RR} + \dot{m}H_w \quad (2)$$

or:

$$C_h (H_{CL} - H_w) = \dot{q}_{RR}(T_w) + \dot{m}H_w \quad (3)$$

in which:

$$H_w = f(B^*, p) \quad (4)$$

as shown in Figure (5).

A comparison of steady state recession rates measured at different facilities and test conditions can be obtained by using the steady state energy balance (Eq. 3) to determine the convective heating rate which must have existed to have produced the measured mass loss rate. This convective heating rate can then be compared with the theoretical value predicted for the given test conditions. If the inferred experimental heating rate exceeds the theoretical value, the degree of augmented heating due to surface roughness can be computed.

Since a quasi-steady shape change is achieved during the steady state tests, the axial recession is equal at all locations on the model surface. Due to difficulties in defining the effective nose radius of the sharpened equilibrium shapes, it is more convenient to work with turbulent heating to the conical region of the model, rather than with laminar stagnation point heating. The theoretical smooth surface turbulent heating transfer coefficient  $C_{h0}$  for a cone is predicted by the Eckert reference enthalpy relation:

$$C_{h0} = \frac{\dot{q}_T}{H_R - H_w} = \frac{.0348}{Pr^{2/3}} (\rho_e U_e)^{0.5} \left( \frac{\mu_e}{S} \right)^{0.2} \epsilon_T \quad (5)$$

The mass loss rate on the conical region is determined by:

$$\dot{m} = \rho \dot{S} \sin \beta \quad (6)$$

in which  $\dot{S}$  is the measured axial recession rate, and  $\beta$  is the cone half-angle. The re-radiation heat flux  $\dot{q}_{RR}$  is computed from the measured surface temperature. Eq. (3) is now used to solve for  $C_h$  by iteration, using Figure 5 to determine  $H_w$  and Figure 4 to determine  $B^*$ . Comparison of  $C_h$  and  $C_{h0}$  yields the augmented heating ratio  $C_h/C_{h0}$ .

The analysis procedure described above was applied to the 124 and 168 atm HIP test conditions, and the 80 atm 50 MW arc test condition, for ablation tests of 3-D carbon-carbon. Local properties needed in evaluating Eq. (5) were determined by isen-

tropic expansion from centerline stagnation conditions to local pressure appropriate to the quasi-steady cone angle for each condition.\* The test conditions selected for the 50 MW arc are representative average values of many runs, while specific runs were selected for HIP tests. The test conditions and calculated values of  $C_{h0}$ ,  $C_h$ , and  $C_h/C_{h0}$  are shown in the following table.

Facility	MEASURED						CALCULATED		
	$P_s$ atm	$H_{CL}$ kJ/kg	$H_{CL}$ btu/lb	$S$ cm/sec	$\beta$ deg	$T_w$ °K	$C_{h0}$	$C_h$	$C_h/C_{h0}$
50 MW	80	11600	5000	.635	45	4000	3.15	4.40	1.4
HIP	124	6914	2980	.508	57	4167	4.56	6.40	1.4
HIP	168	8027	3460	.787	57	4167	5.86	8.80	1.5

It is seen that a consistent degree of augmented heating is inferred from the measured recession rates and wall temperatures for the three different test conditions.

The values of  $C_h/C_{h0}$  computed above should be regarded as first approximations, due to the inherent uncertainties in test conditions. The effects of relaxing some of the assumptions made in the analysis are summarized below.

<u>Assumption</u>	<u>Effect of Relaxing Assumption</u>
• No thermomechanical loss	Finite thermomechanical loss yields lower $C_h/C_{h0}$
• "Standard" $H_{CL}$	Lower $H_{CL}$ yields higher $C_h/C_{h0}$ e.g., $H_{CL} = 8120$ kJ/kg (3500 btu/lb) yields $C_h/C_{h0} = 1.9$ instead of 1.4 for 50 MW arc.

#### RAMP TESTS

The ramp test technique has become a standard test procedure in the 50 MW arc, and has also been used at the HIP facility. Typical determination of transition pressure is shown in Figure 6. By using three cameras, transition can be observed on 6 rays for each model, as inferred from the onset of gouges in the profile.

The results of simply averaging the recorded transition pressure according to camera view are shown below for two test series.

\*A mass balance calculation showed that the boundary layer on the cone surface is fed by a small central core (.061 cm radius for HIP at 168 atm, .112 cm for 50 MW arc at 80 atm), such that centerline stagnation conditions are a reasonable approximation.

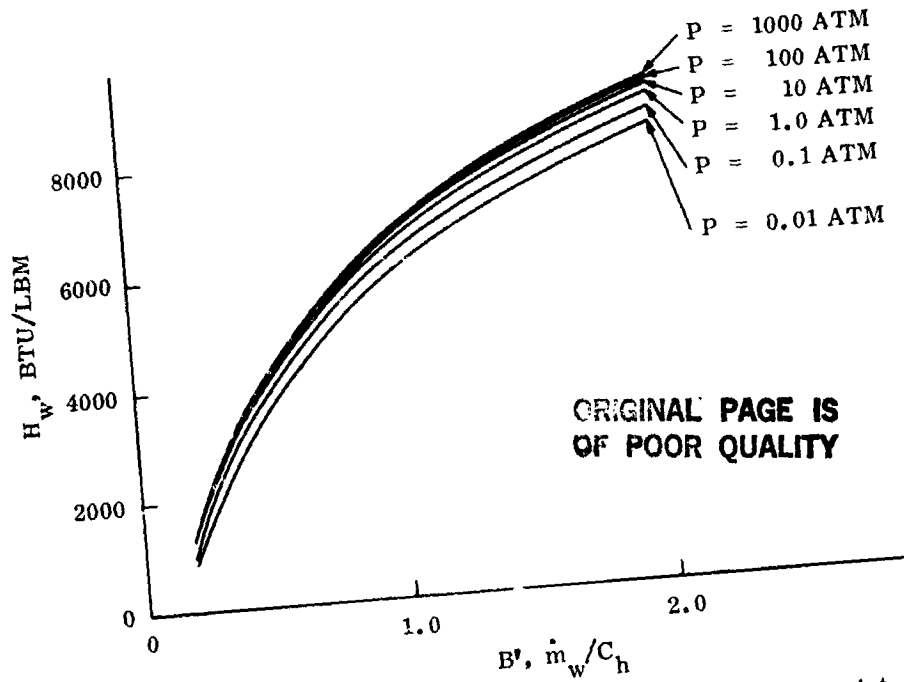


FIGURE 5.  $H_w$  vs.  $B'$  for JANAF (Aerotherm) Thermochemist

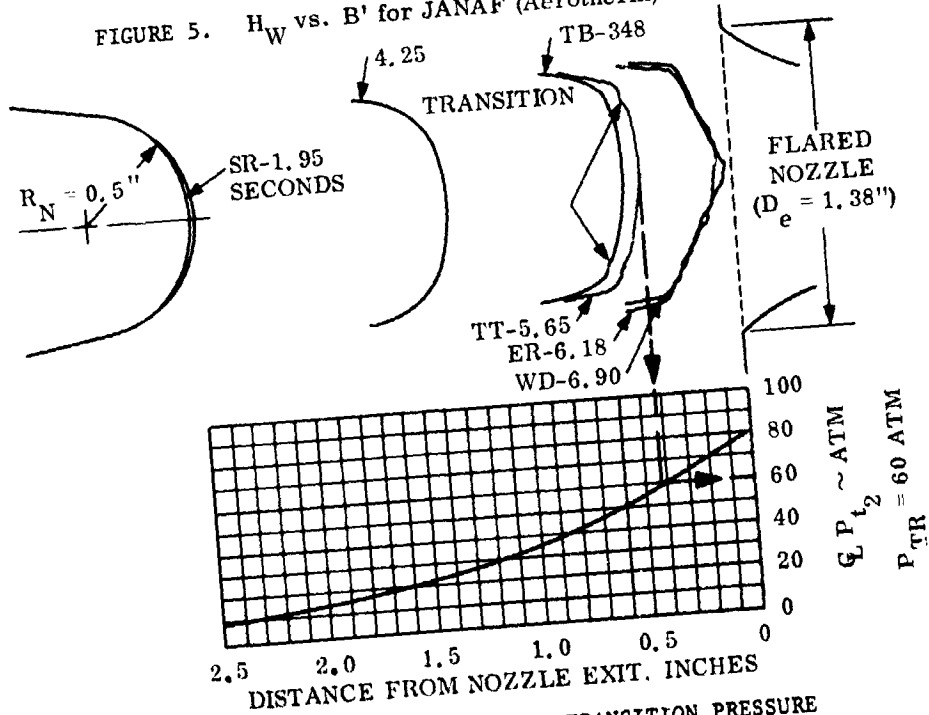


FIGURE 6. TYPICAL DETERMINATION OF TRANSITION PRESSURE

Test Series	North & South Cameras (45° Between Weave Axes)		Top Camera (Along Weave Axes)	
	# Readings	Avg. P <sub>TR</sub> (atm)	# Readings	Avg. P <sub>TR</sub> (atm)
A	38	71.6	20	77.7
B	24	73.5	10	77.4

A clear bias is seen to exist for transition to occur earlier (lower P<sub>TR</sub>) along the 45° direction between weave axes.

A study of transition gouges occurrence from post-test examination of a group of models also showed a consistent bias for transition to occur more frequently on 45° rays (Figure 7), in agreement with previous results of Heinonen and Jumper (Ref. 1). This non-axisymmetric character of transition is due to the three-dimensional weave geometry of carbon-carbon, and is typified by the post-test view of the model shown in Figure 8.

The numerical values of transition pressure given above are typical of good quality processing for a particular 3-D carbon-carbon. Figure 9 shows the decrease in transition pressure which occurs as the open porosity of the test specimen is increased. It appears that the transition pressure can be controlled by varying the open porosity of the material.

#### COMMENTS ON ADEQUACY OF TEST SIMULATION

In any ground test designed to simulate flight conditions, the question arises: is the simulation adequate? In the present case, the 50 MW and HIP arcs provide a high pressure, high enthalpy environment in which comparative performance of material candidates is obtained; hence, exact simulation would appear to be of secondary importance. However, the lack of one-to-one similitude in certain parameters which may be significant in ablation performance suggests the need for caution in interpreting even comparative arc test results. In the following paragraphs, comments are given concerning the adequacy of test simulation for steady state and ramp tests, followed by recommendations for facility developments which would provide improved simulation capability.

#### Steady State Simulation

Recession rates obtained in steady state tests reflect the combined effects of thermochemical and thermomechanical material removal. The simulation of ablative performance of purely thermochemical nature would appear to be adequate for comparative assessment; however, a subtle difference in arc and flight flow field character may result in larger differences in flight performance. Specifically, the different degrees of nose sharpening associated with different surface roughness has little effect on turbulent forecone heating in a low supersonic environment such

ORIGINAL PAGE IS  
OF POOR QUALITY



FIGURE 8. POST-TEST PHOTOGRAPH OF 50 MM ARC  
RAMP TEST MODEL

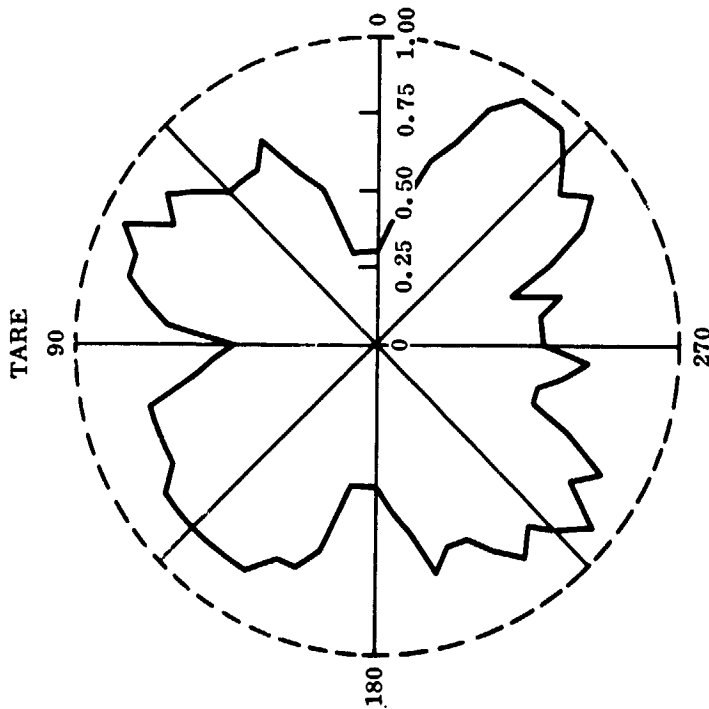


FIGURE 7. FREQUENCY OF TRANSITION VS. CLOCK ANGLE  
13 MODELS

as that of the arcs, but has a large effect in hypersonic re-entry due to the bow shock curvature-streamline swallowing phenomenon illustrated in Figure 10.

Thermomechanical contribution to recession rate at a given test condition is properly simulated only if the full scale nose-tip is tested. The test models in the arcs are smaller than flight nosetips, particularly for the HIP facility where pressure is more representative of re-entry. Local dynamic pressure along the biconic turbulent ablated shape will be lower in arc tests than in re-entry, for common stagnation pressure, due to flow field effects (supersonic vs. hypersonic freestream Mach number). Thus, pressure gradient forces ( $dp/ds$ ) will be larger in arc tests than in re-entry; while dynamic pressure and shear forces will be smaller. Hence, differences in recession rate between two materials may be obtained in arc tests which will not occur in flight.

#### Transition Simulation

Boundary layer transition on a nosetip may be effected by the following variables:

$K/\theta$	relative roughness
$T_w/T_e$	wall-to-stream temperature ratio
$B'$	dimensionless blowing parameter
$E$	dimensionless pressure gradient parameter (Euler number)
$T_u$	turbulence level

Comparison of arc and flight environments is given below.

	Typical Re-entry	50 MW Arc (80 atm)
$P_s$ (atm)	80 - 150	80
$H_{CL}$ (kJ/kg)	9280 - 18560	11600
(btu/lb)	4000 - 8000	5000
$(K/\theta)_{K=0.0025 \text{ cm}}$ (1 mil)	3 to 8	3.0
$T_w/T_e$	0.6 to 1.3	0.7
$Re^*/ft \times 10^6$	5 to 20	8.0
$B'$	0.2 to 0.5	0.4
$E$	Arc higher than re-entry due to radial gradients in approach flow	
$T_u$	Arc higher than clear-air re-entry	

It is seen that reasonably good simulation of several parameters which affect transition is achieved by the arc test conditions, except for  $E$  and  $T_u$ . Also, an indirect influence of pressure and enthalpy on roughness height of the ablating surface may have significance, since the arc values are on the low

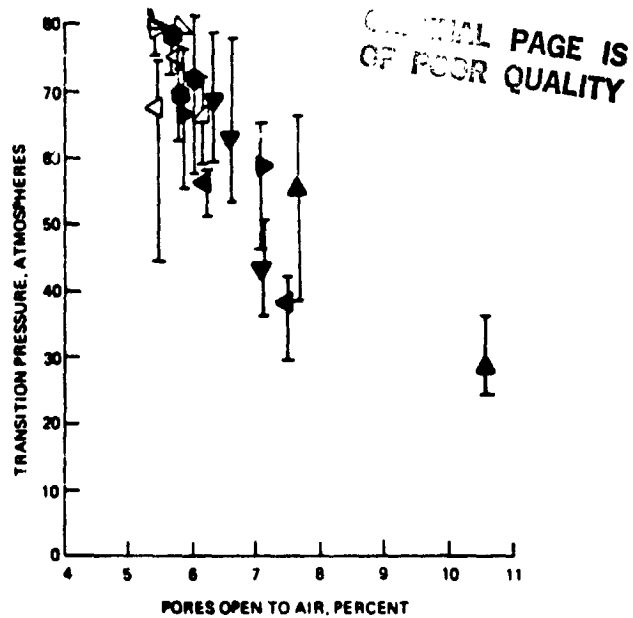


FIGURE 9. TRANSITION PRESSURE VS. OPEN AIR POROSITY

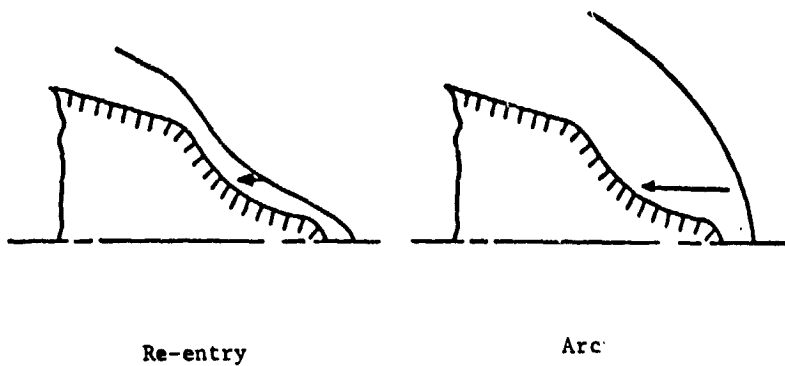


FIGURE 10. ARC SIMULATION DEFICIENCY OF OBLIQUE SHOCK STREAMLINE SWALLOWING

end of the re-entry values.

Differences in arc and re-entry environment can result in different comparative transition performance between two materials. For example, if freestream turbulence controls transition in arc tests (as it may for smoother materials), little difference in transition pressure may be observed; yet during clear air re-entry, larger differences in transition may result because surface roughness controls transition.

#### Facility Recommendations

It is obvious that the ideal facility should provide high enthalpy, uniform low turbulence approach flow, hypersonic Mach number, and a large enough nozzle to test full scale nosetips. Since such a facility is not likely in the foreseeable future, more practical specific recommendations are given below for improved arc test simulation of nosetip ablative performance.

- Reduce the freestream turbulence level by use of a stilling chamber, and observe the affect on transition pressure.
- Provide a moderate increase in pressure-enthalpy-nozzle diameter (model size) similitude, such that variation in test model diameter could be accomplished at a given test condition.
- Provide a thorough calibration of the arc, including measurement of radial and axial gradients of flow properties. This information would permit application of nose shape change computer codes to extrapolate differences in ablation performance in arcs to re-entry conditions.

#### CONCLUDING REMARKS

An evaluation of typical high pressure arc test results for 3-D carbon-carbon nosetip models has demonstrated that steady state recession rates over a wide range of test pressures show a consistent degree of augmented heating due to surface roughness. The non-axisymmetric nature of boundary layer transition has been quantified. The test simulation has been assessed to be reasonably adequate, with the exception of thermomechanical contribution to ablation, and arc freestream turbulence effects on transition.

#### REFERENCES

1. Heinonen, E.W., and Jumper, G.Y., Jr., "A Method for the Evaluation of Damage on the Surface of Carbon-Carbon Ablation Samples", Proc. of Eighth Conf. on Space Simulation, NASA SP-379, Nov., 1975.